CONDENSED-STATE PHYSICS

STRUCTURE AND PHASE COMPOSITION OF A COATING SYNTHESIZED FROM Ti–Ni–Ti LAMINATE ON TiNi SUBSTRATE

E. S. Marchenko,[1] Yu. F. Yasenchuk,[1] S. V. Gunther,[1] G. A. Baigonakova,[1]
O. V. Kokorev,[1] A. A. Shishelova,[2] and O. A. Fatyushina[3]

UDC 538.971

A gradient magnetron-sputtered three-layer laminated Ti–Ni–Ti *coating is formed by the method of reaction synthesis on a titanium nickelide substrate. The resulting coating is designed for investigating the features of formation of the structure and phase composition in the coatings synthesized by self-propagating high-temperature synthesis in order to improve corrosion resistance of* TiNi-*implants. A comparative assessment of the as-formed and coated specimens demonstrates that nanocrystalline titanium oxycarbonitride layers present in the coating effectively improve its cytocompatibility.*

Keywords: TiNi, gradient crystalline coating, laminate, synthesis, structure, diffusion.

INTRODUCTION

The alloys based on TiNi are common biomaterials used in various areas of medicine due to their shape memory property, superelasticity and good biocompatibility [1–3]. Porous TiNi-alloys produced by the method of self-propagating high-temperature synthesis (SHS) possess high corrosion resistance [4, 5]. In the course of SHS in an argon and nitrogen flow, thin and dense gradient layers of intermetallic carbides and nitrides are formed on the alloy surface, which improve its corrosion resistance without suppressing the superelasticity and shape memory effects [6, 7]. An investigation of the mechanisms of corrosion resistance and phase and elemental compositions of the porous alloy surfaces is complicated by their intricate relief and inconvenient access to the surface. It is preferable to investigate the phase formation and corrosion resistance of the surface using a flat TiNi-substrate. To do so, it is necessary to form a model coating by the SHS method. These methods are well known and are used in engineering.

Intermetallic coatings synthesized using a preliminary plasma deposition of multiple layers of the reaction components are widely used as a reliable protection of machine parts and components from thermal stresses and corrosion attacks [8–13].

In the recent decade this method has been most actively developed in microelectronics for soldering and welding of the temperature-sensitive components, where it coined its current name – Reactive Multilayer Systems (RMS). An advantage of the RMS is a local heat release due to self-propagation of the local reaction zone, which allows decreasing heating of the joined plates. The RMS approach is implemented in a pack of alternating nanosized layers of exothermally reacting materials, generating a self-propagating reaction front at room temperature [8–10]. A fusion
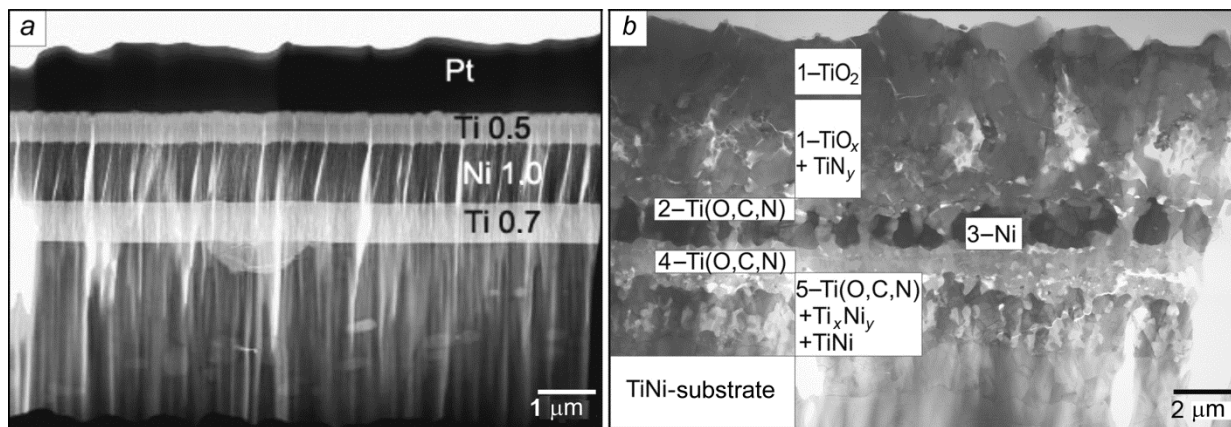
Fig. 1. TEM images of Ti–Ni–Ti layers deposited on a TiNi substrate in argon (*a*) and the resulting gradient crystalline coating synthesized in air (*b*).

reaction is initiated by an external power source, such as an electric spark. After initiation, the reaction propagates along the deposited layers due to the heat released by the exothermal reaction and heat conduction of the layers.

The RMS approach has certain specific features. Due to interdiffusion of the alternating components during diffusion, a mixed layer is formed at the phase boundaries, which reduces the reaction exorthermicity and increases the synthesis reaction activation energy.

A number of models were developed in numerous studies, which are used to investigate the temperature-dependant heat conduction effects and melting of multilayered materials [11–13].

The purpose of this study is to investigate a gradient coating on a flat TiNi substrate, formed by the reaction synthesis of a Ti–Ni–Ti laminate in an air medium.

EXPERIMENTAL MATERIALS AND PROCEDURES

In order to get an opportunity of a more convenient investigation of the resulting coating the process of the surface layer synthesis was modeled on a flat TiNi substrate. A multiple-layer intermetallic coating was manufactured by depositing a three-layer Ti–Ni–Ti laminate on the substrate, followed by heating of the specimen in air. This approach allowed investigating the process of phase formation both on the outer surface and at the phase boundaries of TiNi–Ti–Ni–Ti.

The alloy based on TiNi was melted in an induction furnace by re-melting of spongy titanium and nickel. The resulting ingots were rolled to form ribbons, followed by cutting 10×10 mm specimens from them. Before deposition, the specimen surfaces were ground using a soft abrasive paper (up to 5000 grit ISO 6344) and etched by an argon plasma ion beam in vacuum of 10^{-5} Pa. During magnetron sputtering of the Ti–Ni–Ti layers in argon, titanium and nickel targets were used. The deposited layer thickness was within 0.5–1.0 µm (Fig. 1*a*). For the reaction synthesis of the coating, the specimen with the deposited laminate was heated in air in a tube-type furnace to a temperature of 950°C and tempered for 60 s.

A 80–60 nm-thick lamel was cut from the specimens in a Quanta 3D 200i microscope in order to monitor the deposited layer thickness and homogeneity, followed by further investigations in a JEOL JEM-2100F transmission electron microscope. Another lamel was cut from the surface part of the specimen using an EM-09100IS Ion Slicer. The latter was investigated in a STEM mode in a JEOL JEM-2100F microscope. The structural-phase composition of the surface was investigated by the X-ray diffraction analysis in a grazing angle geometry at a tilt angle of 3° in an XRD-6000 diffractometer in the CuK_α emission. The XRD patterns were interpreted using a POWDER CELL 2.4 full-profile analysis software program. The cytotoxicity of the synthesized coating was evaluated by a quantitative index of the cell culture viability using an MTT-test.

1790

RESULTS AND DISCUSSION

The laminated layers were formed on a TiNi substrate in two stages. In the first stage three Ti–Ni–Ti layers were successively deposited and their thicknesses were 0.5–1.0–0.7 µm, respectively. The layer thickness was chosen based on the purpose of investigating the phase transformations quite noticeable in thick layers. Recall that for an implant to function under the conditions of alternating deformation it is inacceptable to have a layer thickness of more than a micron, since a thick coating is prone to crack formation. Therefore our case is a model case belonging to the upper bound of the total thickness; in our further work the layer thickness will be reduced.

For the sake of monitoring the thickness and structure of the deposited layers, a lamel was cut from the specimen surface by an argon plasma beam in a Quanta 3D 200i microscope. Before cutting the specimen surface was protected with a Pt layer (Fig. 1*a*). Prior to cutting the deposited layers were sustained in an amorphous state.

In the second stage, a spontaneous exothermal reaction of synthesis took place between the laminate layers after heating the specimen to 950°C. As a result of the reaction, the former trilayer laminate transformed into a pentalayer crystalline coating (Fig. 1*b*). This is indicated by the granular structure of the layers and also additional fine-grained layers at the layer interfaces. Due to the interstitial impurities of nitrogen, carbon, and oxygen at the phase boundaries of the deposited layers Ti (1), Ni (3), Ti (5), nanocrystalline barrier layers were formed (2 and 4), which limit interdiffusion in the Ti–Ni–Ti laminate and prevent the layer intermixing. It is for this reason that the nickel and titanium layers crystallized independently without forming a homogeneous intermetallic phase.

Upon heating to 950°C, the outer titanium layer 1 was subjected to intensive oxidation resulting in the formation of a thick oxide layer. It should be noted that in contrast to a considerable increase in the outer titanium layer thickness, the inner titanium layer adjacent to the substrate did no demonstrate any growth. Presumably, the volumetric growth of the new crystalline phase in the outer layer had occurred due to a large number of impurities, whose transport to the inner titanium layer is strongly limited. It can be assumed that the new crystalline phase in the outer layer is predominantly formed by titanium oxycarbonitrides.

In addition, the nickel layer 3 decreased in its volume due to its crystallization. The monolithic deposited amorphous nickel layer lost continuity in the course of heating and crystallization and decreased in its thickness from 1.0 to 0.7 µm. The crystalline monolithic nickel layer consists of coarse crystals measuring about 0.4 µm and characterized by a block structure, where the spaces between the blocks are filled with fine titanium oxycarbonitride crystals about 0.2 µm in size.

An energy dispersive elemental analysis has demonstrated that layer 4 consists of nanocrystals of titanium carbides and nitrides containing dissolved oxygen and is in fact a titanium oxycarbonitride layer (Fig. 2). For titanium, the formation of a volumetric phase of titanium oxycarbonitride in the deposited titanium layer seems to be a priority process – it inhibits interdiffusion between Ti and Ni through the phase boundary and prevents the formation of Ti_2Ni, TiNi, and $TiNi_3$ intermetallic compounds. The average grain size of titanium oxycarbonitride in the nanocrystalline layer 4 is found to be 20–70 nm. This layer is the first to be synthesized primarily due to the availability of interstitial impurities in the mixed Ti+Ni region formed as early as during deposition, which is activated in the course of heating.

There is a certain degree of nickel diffusion along the crystal boundaries, since it is found in minor amounts between the grains of titanium oxycarbonitride. The interdiffusion of nickel and titanium, which generally results in the formation of intermetallic compounds upon heating the diffusion pairs, is in our case minimal – it has brought about the formation of a 10 nm-thick intermetallic TiNi interlayer at the interface between layers 3 and 4.

It is evident in the TEM-image that a wide about 2 µm-deep heat-affected zone has formed, which consists of columnar crystals and can ensure strong bonding with the substrate (Fig. 1*b*).

An XRD analysis (Fig. 3) has demonstrated that the oxide layer at a depth of 300 nm consists of titanium dioxide of various modifications of the tetragonal and monoclinic crystallographic systems. The main structure component of the surface layer is a TiO_2-phase in a rutile modification giving high-intensity diffraction reflections, whose volume fraction is up to 60%. This is in a good agreement with the works by other authors on oxidation of titanium alloys at the temperature above 500°C in air, in which case the rutile phase is the main stable form of TiO_2 after its transformation from anatase and brookite [14]. The broadened diffraction reflections result from superposition and overlapping of the TiO_2 phase reflections and small crystallite dimensions, which correlates with the calculated CSR size not exceeding 70 nm for all identified phases.
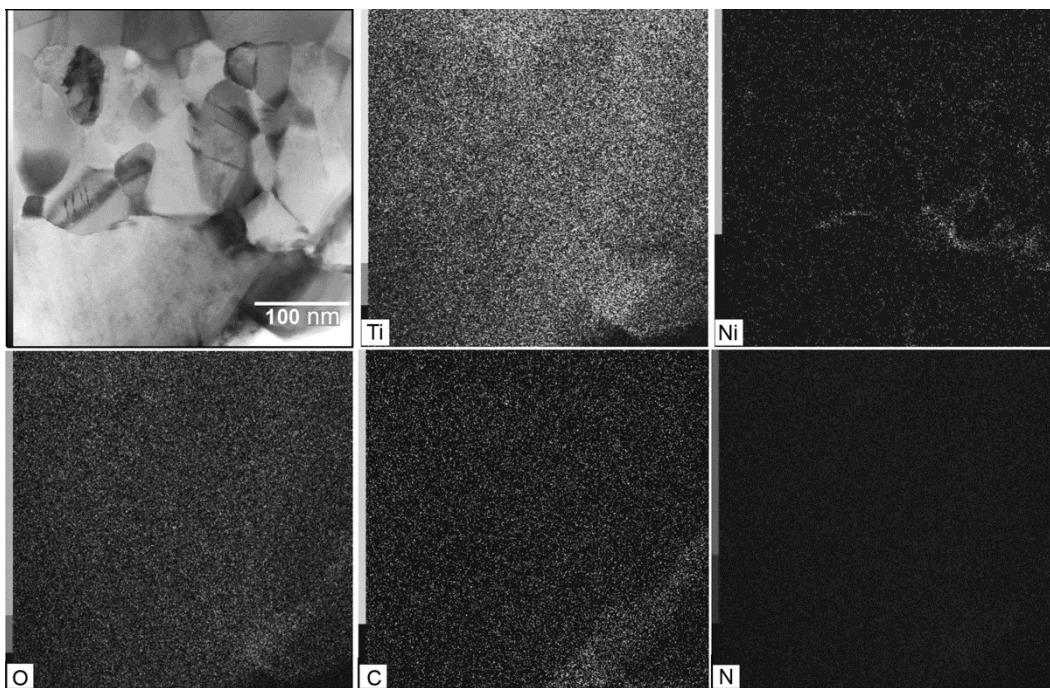
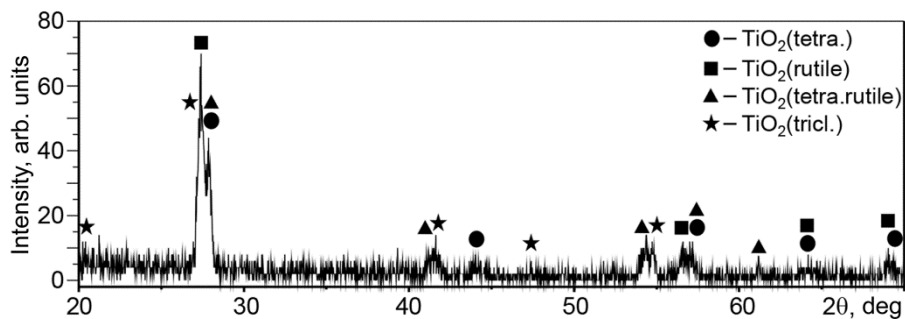Fig. 2. TEM and energy dispersive elemental analyses of the 4-th nanocrystalline layer.

Fig. 3. X-ray pattern from the surface of a Ti–Ni–Ti laminated coating formed on a TiNi substrate.

It is well known that oxide and oxinitride titanium coatings exhibit excellent biocompatibility properties [14, 15]. A direct method for evaluating their biocompatibility is settling of cells onto the surface, followed by an investigation of their adhesion. An assessment of biocompatibility properties of the synthesized coating was performed by inoculating thrombocytes on the coated and uncoated specimen surfaces, calculation of the number of cells per unit area and evaluation of the cell appearance in the proliferating stage.

A high-density homogeneous distribution of the cell mass has been revealed on the modified surface, showing high proliferating capacity (Fig. 4). No cell proliferation has been observed on the reference alloy specimen.

CONCLUSIONS

1. By the method of XRD analysis it has been found out that the synthesized surface layer of the coating at a depth up to 300 nm is entirely crystalline and consists of a TiO_2 group with monoclinic and tetragonal lattices. The CSR dimensions for detection of oxide phase are found to be 50–70 nm.
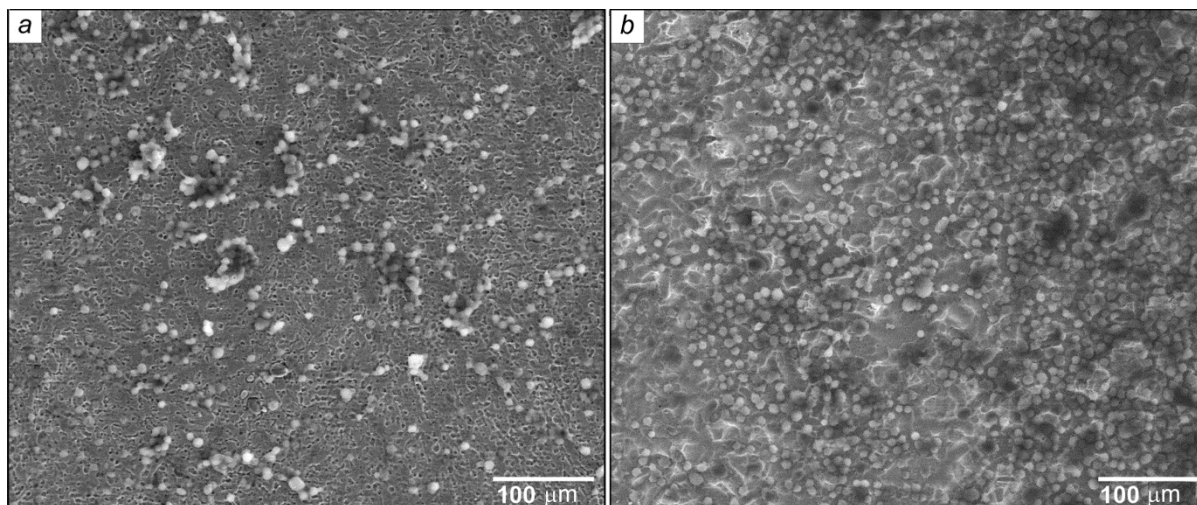
Fig. 4. External view of the coated and uncoated specimen surfaces after their inoculation with the cell cultures.

2. At the nickel – titanium interface a nanocrystalline layer has formed, which inhibits the nickel – titanium interdiffusion.

3. The coated specimen has demonstrated the best cytocompatibility of thrombocytes due to the fact that the synthesized nanocrystalline layers of titanium oxycarbonitride prevent nickel from diffusing to the surface.

REFERENCES

1. T. Yoneyama and S. Miyazaki, Shape Memory Alloys for Biomedical Applications, Woodhead Publishing Limited (2009).
2. Yu. Yasenchuk, E. Marchenko, V. Gunther, *et al*., Materials, **12**, 2405 (2019).
3. A. I. Potekaev, A. A. Klopotov, and A. N. Matyunin, Inorgan. Mater.: Appl. Res. , **2**, No. 4, 387–394 (2011).
4. F. M. Braz Fernandez, Shape Memory Alloys. Processing, Characterization and Applications, Intech, Portugal (2013).
5. DA. Jones, Principles and Prevention of Corrosion (2nd ed.), Prentice Hall, Upper Saddle River (1996).
6. O. V. Kokorev, V. N. Khodorenko, G. A. Baigonakova, *et al*., Russ. Phys. J., **61**, No. 9, 1734–1740 (2018).
7. V. Gunther, Y. Yasenchuk, T. Chekalkin, *et al*., Adv. Powder Technol., **30**, No. 4, 673–680 (2019).
8. T. W. Barbee and T. P. Weihs, Ignitable heterogeneous stratified structure for the propagation of an internal exothermic chemical reaction along an expanding wavefront and method of making same, US Patent No. 5538795A (07 July 1996).
9. J. C. Trenkle, J. Wang, T. P. Weihs, and T. C. Hufnagel, Appl. Phys. Lett., **87**, No. 15, 153108 (2005).
10. E. Besnoin, S. Cerutti, O. M. Knio, and T. P. Weihs, J. Appl. Phys., **92**, No. 9, 5474–5481 (2002).
11. M. Salloum and O. M. Knio, Combust. Flame, **157**, No. 2, 288–295 (2010).
12. L. Alawieh, O. M. Knio, and T. P. Weihs, J. Appl. Phys., **110**, No. 1, 013509 (2011).
13. F. Baras and D. Kondepudi, J. Phys. Chem., **111**, No. 23, 6457–6468 (2007).
14. I. A. Khlusov, V. F. Pichugin, A. A. Pustovalova, *et al*., Bull. Sib. Med., **14** , No. 2, 55–66 (2015).
15. F. Lopez-Huerta, B. Cervantes, O. Gonzalez, *et al*., Materials (Basel), **7**, No. 6, 4105–4117 (2014).